IIETA International Information and Engineering Technology Association
Advancing the World of Information and Engineering

Annales de Chimie - Science des Matériaux
Vol. 47, No. 6, December, 2023, pp. 399-404
Journal homepage: http://iieta.org/journals/acsm

Synthesis of Polyaniline-Zinc Oxide Composites: Assessment of Structural, Morphological, and Electrical Properties

Mohamed Yacine Tababouchet[1,2*], Adel Sakri[2,3], Cherifa Bouremel[2,3], Ahmed Boutarfaia[2,3]

[1] Department of Science and Techniques, University of Bordj Bou Arréridj El-Anasser, El-Anasser 34030, Algeria
[2] Applied Chemistry Laboratory, University of Biskra, Biskra 07000, Algeria
[3] Department of Industrial Chemistry, University of Biskra, BP 145 RP Biskra 07000, Algeria

Corresponding Author Email: yacine.tababouchet@univ-bba.dz

https://doi.org/10.18280/acsm.470606

Received: 29 December 2022
Revised: 21 October 2023
Accepted: 31 October 2023
Available online: 22 December 2023

Keywords:
conductivity, FT-IR, in-situ oxidative polymerization, polyaniline, Scanning Electron Microscopy (SEM), X-ray diffraction, zinc-oxide

ABSTRACT

In this study, nanocomposites of polyaniline-zinc oxide (PANI-ZnO) were synthesized via in-situ chemical oxidative polymerization, employing ammonium persulfate [$(NH_4)_2S_2O_8$] as an oxidant in an acidic milieu. Variations in zinc oxide content (1%, 3%, and 5%) were systematically explored. Comprehensive structural and morphological evaluations were conducted utilizing Fourier-transform infrared spectroscopy (FT-IR), X-ray diffraction (XRD), and scanning electron microscopy (SEM). The integration of ZnO was found to facilitate hydrogen bond formation with the N-H groups of PANI, a phenomenon consistently observed across all composites. Notably, ZnO incorporation induced morphological transformations and fostered crystallite growth, with dimensions expanding from 10.8 nm to 21.8 nm. These structural alterations were also reflected in the diverse morphologies of the resultant composites. The electrically conductive properties, assessed via the four-point probe method, revealed a significant enhancement in conductivity, achieving values as high as 1.65×10^{-2} S.cm^{-1}. The study establishes a direct correlation between the ZnO content and the resultant conductivity, underscoring the potential of PANI-ZnO composites for advanced applications in fields demanding high electrical conductivity, including but not limited to sensors, energy conversion systems, smart textiles, and electrochromic devices.

1. INTRODUCTION

Recent decades have witnessed a burgeoning interest in the realm of electrically conducting polymers, with a considerable focus on their derivatives by the electrochemical research community, attributable to their intriguing physical and chemical attributes [1]. Conducting polymers, characterized by rapid charge transfer, elevated ionization potentials, and outstanding resistance to corrosion, have emerged as viable candidates for a spectrum of electrochemical applications. These include energy storage systems, catalytic processes, and sensor technologies, with their ease of production, affordability, and environmental compatibility further augmenting their appeal [2-5]. Among these, polyaniline (PANI) has been extensively investigated and employed across a diverse array of technological implementations due to its superior chemical and structural characteristics [6]. The utility of PANI spans a wide range of applications—from nanoelectronic devices to actuators, and from rechargeable batteries to supercapacitors, catalytic agents, and sensors, underscoring the necessity to continually enhance its properties [7-9]. Recent scholarly endeavors have pivoted towards the development of heterogeneous conductive polymer nanocomposites, with a specific interest in the synergy between organic and inorganic materials [10].

In light of the aforementioned properties of conducting polymers, the incorporation of nanoscale additives has been recognized as an essential strategy to augment the electrical properties of host materials such as polyaniline [11]. Zinc oxide (ZnO), a member of the II-VI semiconductor family, is distinguished by a direct band gap of 3.37 eV, rendering it suitable for integration into electronic devices [12, 13]. The attributes of ZnO—encompassing high electron mobility, chemical stability, non-toxicity, mechanical robustness, and an expansive surface area when in powdered form—have been exploited to enhance the performance and broaden the utility of various electronic components [14-16].

Several synthesis methods for PANI/ZnO nanocomposites are prevalent, with in-situ polymerization, direct mixing, and template synthesis standing out due to their efficacy in the production of polymer nanocomposites [17]. In-situ polymerization, in particular, has been employed for its ability to integrate nanomaterials into a polymerizing solution of monomers, resulting in covalent bonding within the matrix [18]. The work by Gilja et al. [19] illustrates the synthesis of PANI/ZnO composites through in-situ oxidative polymerization, although the resulting composite demonstrated limited conductivity of 1.862×10^{-6} S.cm^{-1}. Contrastingly, the research by Vijayalakshmi et al. [5] highlights the successful synthesis of a PANI/ZnO

nanocomposite with 10 wt% ZnO through in-situ polymerization in an HCl medium, achieving a considerably higher conductivity of 4.35×10^{-3} S.cm^{-1}.

The current study advances this field by presenting the synthesis of PANI-ZnO nanocomposites with a systematic variation of ZnO nanoparticle concentrations within the PANI matrix. In-situ oxidative polymerization in a sulfuric acid milieu was utilized to identify the optimal ZnO ratio for enhancing the conductivity of the composite. A suite of analytical techniques, including SEM, FT-IR, and XRD, were employed to investigate the impact of ZnO on the morphology, structural integrity, and crystallinity of the composites. The synthesized nanocomposite exhibited a significant elevation in electrical conductivity, attaining a value of 1.65×10^{-2} S.cm^{-1}, which is markedly superior to that of pristine PANI.

2. MATERIALS AND METHODS

PANI-ZnO nanocomposite samples were prepared via in-situ oxidative polymerization from aniline. The polymerization occurred in an acidic medium in the presence of ZnO nanoparticles and ammonium persulfate as an oxidizing agent. 11 g of ammonium persulfate [$(NH_4)_2S_2O_8$] were dissolved in 50 ml of sulfuric acid (pH=1) with 1 wt% ZnO nanoparticles to obtain an oxidizing solution. The mixture was then put into a dropping funnel. 4.65 g of aniline were dissolved in a flask containing 100 ml of sulfuric acid. After that, ice was used to cool the flask to the target synthesis temperature of 5°C. Once this temperature was reached, the oxidizing solution was added dropwise through the dropping funnel, ensuring that the temperature remained constant by the continuous addition of ice. The mixture was stirred for 1 hour after the contents of the flask were poured out. It should be noted that, initially, the mixture had no color. Subsequently, after 3 to 5 minutes, it became colored, and finally, a colloidal solution was obtained, accompanied by a dark green precipitate. The precipitate was then cleaned using sulfuric acid and distilled water and filtered under vacuum conditions. Finally, it was dried to a constant weight in an oven for 48 hours at 50°C. Using the same procedure previously described, several PANI-ZnO nanocomposite samples are prepared by incorporating ZnO into the aniline monomer at weight ratios of 1%, 3%, and 5%.

3. RESULTS AND DISCUSSION

3.1 X-ray diffraction analysis

The XRD analysis was first used to examine the structure of the polyaniline and the polyaniline–ZnO composites and then to investigate the effect of different amounts of zinc oxide (ZnO) on the structure and crystallite size of polyaniline. Furthermore, the shape of the peaks located in the 2-theta angle range between 10° and 30°, as illustrated in the DRX diffractogram (Figure 1), shows that the product analyzed is amorphous, which is in agreement with the literature, which has confirmed that the polyaniline polymer is amorphous [20]. Within the aforementioned wide characteristic, we can also see peaks at 2-theta angles of around 20.19° and 25.13°; these two peaks display reflections from the planes (020) and (200), indicating the partially crystallized emerald salt form of polyaniline [20, 21]. with the d spacing respectively equal to 4.39 Å and 3.54 Å. The XRD pattern clearly shows low crystallinity of the conductive polymers due to the repetition of benzenoid and quinoid rings in the polyaniline chains [22, 23]. Similar patterns may be seen in all polyaniline-ZnO composites, including the large peak of amorphous polyaniline (18°-28°). However, when the amount of ZnO oxide in the PANI-ZnO composite increases, their intensity increases, indicating that ZnO nanorods and PANI interact through the creation of hydrogen bonds between H-N and the oxygen in ZnO [23]. Depending on the proportion of the doping Zinc oxide, the diffractogram of the polyaniline-ZnO composite depicts tiny peaks corresponding to ZnO plane (100) (002) and (101) [24, 25] (with 3% and 5% wt), in addition to a broad characteristic related to polyaniline. These results ideally match the expected ones.

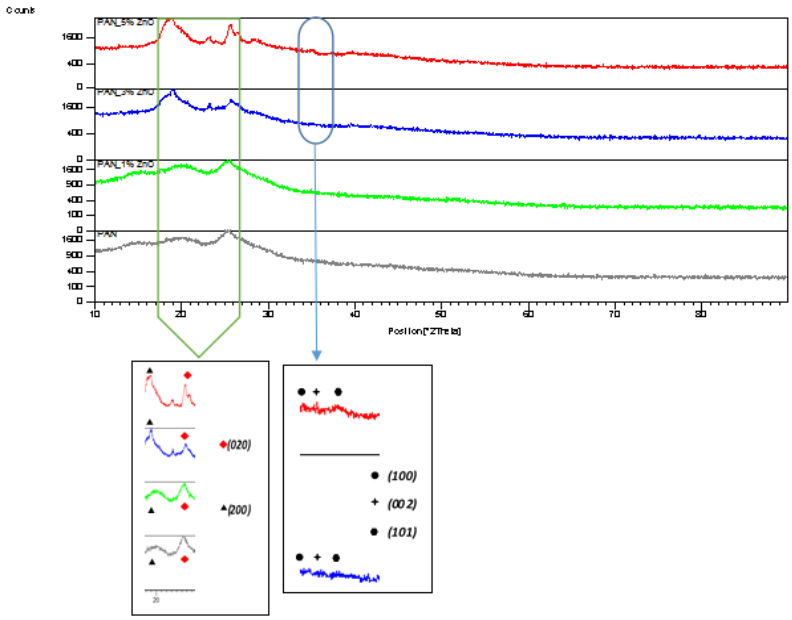

Figure 1. XRD spectra of synthesized PANI and PANI-ZnO nanocomposite

In addition, The Scherrer formula was used to calculate the crystallite size of both PANI and PANI-ZnO nanocomposites, which was 10.8 nm for the PANI. In the presence of ZnO, it was found that the crystallite size increased from 10.8 nm for polyaniline alone to 18.1 nm and 21.8 nm for the 1% and 3%, polyaniline-ZnO composite respectively, indicating that increasing the amount of ZnO into polyaniline increases the crystallite size which then becomes constant as it reaches the maximum value 21.8 nm, corresponding to the addition of 3% and 5% of ZnO into polyaniline.

The Table 1 provides the detailed results of the X-ray diffraction analysis of PANI and PANI-ZnO nanocomposite. From these results, the lattice parameters and crystallite size of PANI, PANI-ZnO (1wt%), PANI-ZnO (3 wt%), and PANI-ZnO (5 wt%) nanocomposites samples are calculated. Based on the results presented in this table, it is observed that the crystallite size of PANI-ZnO nanocomposite samples increases with the increase of the amounts of ZnO in PANI.

Table 1. XRD analysis properties and crystallite size evaluation

Products	Hkl	Position (2theta)	FWHM [°2theta]	d-Spacing [Å]	Intensity (cts)	Crystallite Size [nm]
Polyaniline	200	25.1337	0.2991	3.54323	1221.74	10.8
	020	20.1911	0.7478	4.39804	774.46	
Polyaniline-(01%) ZnO	200	25.5103	0.4487	3.49177	1199.14	18.1
	020	19.2786	0.4487	4.6041	814.84	
Polyaniline-(03%) ZnO	200	25.7496	0.3739	3.45987	1089.11	21.8
	020	19.088	0.3739	4.64964	1697.47	
	100	31.4112	0.0374	2.84798	77	
	002	35.0944	0.4487	2.55706	54.08	
	101	36.5035	0.0561	2.46152	92.59	
Polyaniline-(05%) ZnO	200	25.5774	0.3739	3.48276	1553.37	21.8
	020	18.9937	0.3739	4.67249	2066.74	
	100	31.5648	0.0561	2.83446	144.3	
	002	34.4417	0.1496	2.60401	58.25	
	101	35.6968	0.0748	2.51528	84.66	

3.2 Scanning Electron Microscopy (SEM)

Figure 2 shows polyaniline and polyaniline-ZnO composite Scanning electron microscopy surface morphologies with different ZnO contents. The SEM image of the pure polyaniline exhibits a flaky-shaped structure with many pores. It also shows a non-uniform morphology, probably due to its weak crystalline characteristics, as confirmed by the XRD analysis.

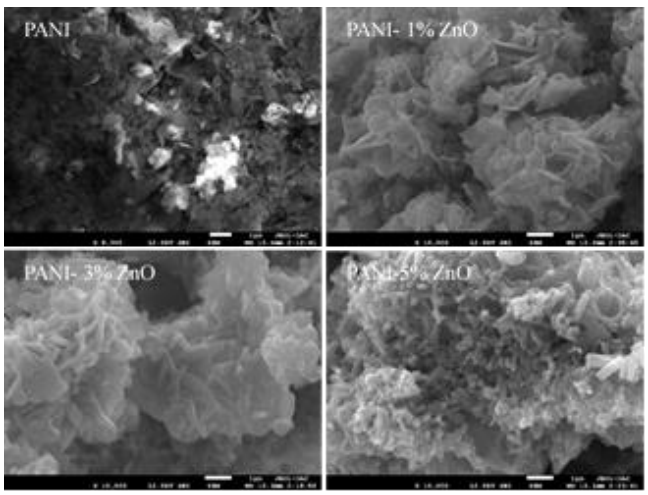

Figure 2. SEM image of synthetized PANI and PANI-ZnO nanocomposite

The image of the nanocomposite PANI-ZnO shows no agglomeration and uniform distribution of the ZnO particles in the PANI matrix. It was observed that the size of flakes decreased as higher percentages of ZnO were added to the reactant mixture for the synthesis of the polyaniline composite. In addition, the difference in size of obtained PANI and PANI-ZnO composites was caused by PANI agglomeration in the presence of Zinc oxide. Increasing the additional amount of ZnO can reduce the PANI size. This agglomeration is caused by hydrogen bonds that occur due to the interaction between ZnO and N-H or coordination bonds [26, 27]. The SEM image helped us to conclude that the increasing ZnO percentage has a significant effect on the morphology of PANI, clearly showing the dual structure of the PANI-ZnO nanocomposite that is comprised of spherical-granular particles and lamellas since PANI has various structures such as nanofiber, nanotubes and flake [26].

3.3 Fourier transform infrared spectroscopy

Pure polyaniline and polyaniline-ZnO composites were structurally characterized using the Fourier transform infrared method. The polyaniline and polyaniline-ZnO composites' FTIR spectra are displayed in Figure 3.

FTIR analysis was also carried out to understand the structure of the PANI and PANI-ZnO nanocomposite. As shown in Figure 4, The major characteristic peaks in PANI obtained at 1581 cm^{-1} and 1507 cm^{-1} were attributed to the C=C stretching vibration of benzenoid and quinoid unite groups, respectively [27]. Additionally, there was a peak present at approximately 3266 cm^{-1} that was attributed to the N-H stretching vibrations [16]. The presence of two peaks with nearly identical intensities, at 1295 cm^{-1} and 695 cm^{-1}, is explained by the (C-N) stretching vibration in the secondary amines' benzenoid ring. On the other hand, the second peak describes the quinoid units' (C=N) stretching vibration. Moreover, the 854 cm^{-1} and 1415 cm^{-1} peaks were associated with aromatic ring C-H stretching vibrations that were outside of the plane as well as in the plane, respectively. Despite this, the FTIR spectrum of the PANI-ZnO nanocomposite (Figure 3) shows similar structural characterization with pure PANI. The absorption band exhibits some displacement when ZnO is added to the PANI. These peaks were shifted to higher wavenumber. The PANI peaks at 1581 cm^{-1}, 1507 $cm^{-1}$and 1363 cm^{-1} are shifted to 1560 cm^{-1}, 1480 cm^{-1} and 1331 cm^{-1}, respectively. These peak shifts characteristic of PANI

nanocomposite may be due to the formation of interactions between the chains of PANI and Zn [28-30]. Moreover, the existence of two peaks at 603 cm^{-1} and 1128 cm^{-1} related to Zn-N stretching frequency and the interaction bond between ZnO and PANI chain [31]; these peaks disappeared in the FT-IR spectrum of pure PANI. He [32], Paul et al. [33] and Patil et al. [34] also observed the interaction between PANi and ZnO particles.

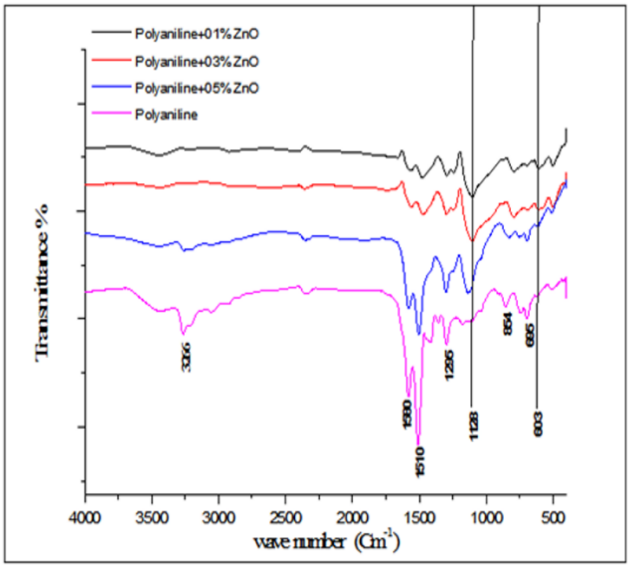

Figure 3. Infrared spectra of synthesized PANI and PANI-ZnO composite

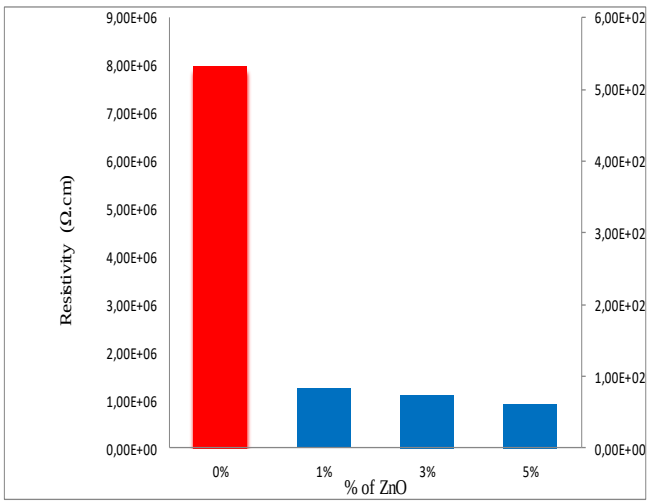

Figure 4. Resistivity of PANI–ZnO with different ratios of ZnO

3.4 Electrical properties

The electrical properties of polyaniline-ZnO composites are illustrated in Figures 4 and 5; these figures present the variation of the resistivity and conductivity as a function of different amounts of the ZnO dopant. The results show that pure PANI has the lowest electrical conductivity (9.15×10^{-7} $S.cm^{-1}$), which increases with the addition of ZnO. In contrast, the conductivity of PANI-ZnO samples reached $1{,}65\times10^{-2}$ $S.cm^{-1}$ conversely for resistivity. It is widely known that the charge transport behaviors of conjugated polymers are highly dependent on the processing parameters. Polyaniline has active N-H groups that are protonated and deprotonated as it adsorbs through nitrogen, which has two free electrons [35], which makes it easier for electrons to move along the chain. On the other hand, adding Zn^{+2} cation to the polymer chain as an extra dopant in the PANI-ZnO nanocomposite supports the network of electrons moving inside the PANI, which makes it more conductive. As mentioned, the conductivity of the polymer depends on the nature of the dopant and the concentration of inorganic materials, which have an essential role in conductivity [23].

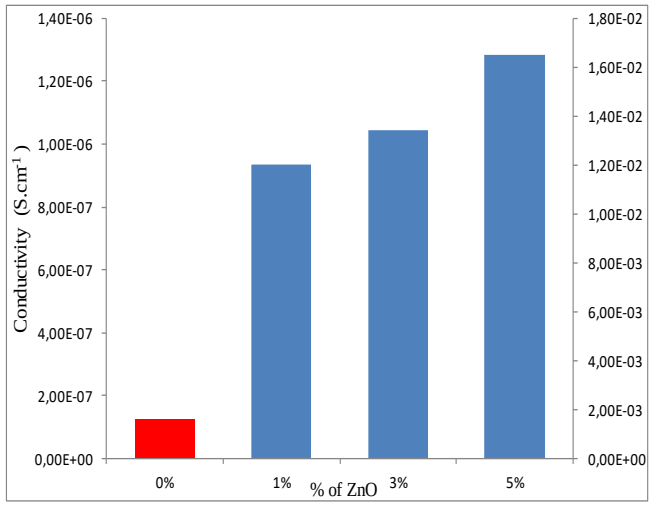

Figure 5. Conductivity of PANI–ZnO with different ratios of ZnO

4. CONCLUSION

Polyaniline-zinc oxide nanocomposites with different ZnO concentrations (1%, 3%, and 5%) were successfully synthesized using the in-situ oxidative polymerization method in an acidic medium with ammonium persulfate. FT-IR spectroscopy, SEM, and XRD were used for detailed analysis. The study's findings lead to the following conclusions:

FTIR spectroscopy analysis confirmed the synthesis of polyaniline and the success of the formation of nanohybrids PANI-ZnO by the interaction that occurred between PANI and ZnO nanoparticles with the appearance of peaks at 1581 cm^{-1}, 1507 cm^{-1}, and 1363 cm^{-1} are shifted to 1560cm^{-1}, 1480 cm^{-1} and 1331 cm^{-1}, respectively, which correspond to the characteristic bands of PANI. The shifting of the prominent peaks is attributed to the formation of interactions between the chains of PANI and ZnO. In addition, XRD patterns revealed a significant increase in the size of the crystallite (10.8 nm to 21.8 nm) with the increase in ZnO content. In accordance with the SEM imaging investigation, the form of the composite's structure varies according to the amount of ZnO present. The texture and appearance of the nanocomposite are significantly influenced by this quantity of ZnO. Interestingly, the structural results of the synthesis process showed a diverse range of shapes for the resulting nanocomposites.

To further investigate the potential benefits of these nanocomposites in practice, we conducted a comprehensive analysis of the electrical properties of the samples. The analysis revealed commendable electrical conductivity properties, reaching a value of $1{,}65\times10^{-2}$ $S.cm^{-1}$ and this qualifies it to be effective in several areas, including sensors, energy harvesting, and various electronic devices.

REFERENCES

[1] Wegner, G. (1981). Polymers with metal-like conductivity-a review of their synthesis, structure and properties. Angewandte Chemie International Edition in English, 5(4): 361-381. https://doi.org/10.1002/anie.198103611

[2] Micaroni, L., Nart, F., Hümmelgen, I. (2002). Considerations about the electrochemical estimation of the ionization potential of conducting polymers. Journal of Solid State Electrochemistry, 7: 55-59. https://doi.org/10.1007/s10008-002-0289-0

[3] Deshpande, P.P., Jadhav, N.G., Gelling, V.J., Sazou, D. (2014). Conducting polymers for corrosion protection: A review. Journal of Coatings Technology and Research 11: 473-494. https://doi.org/10.1007/s11998-014-9586-7

[4] Khomenko, V., Frackowiak, E., Barsukov, V., Béguin, F. (2006). Development of supercapacitors based on conducting polymers. In New Carbon Based Materials for Electrochemical Energy Storage Systems: Batteries, Supercapacitors and Fuel Cells, pp. 41-50. https://doi.org/10.1007/1-4020-4812-2_4

[5] Vijayalakshmi, S., Kumar, E., Ganeshbabu, M., Venkatesh, P.S., Rathnakumar, K. (2021). Structural, electrical, and photocatalytic investigations of PANI/ZnO nanocomposites. Ionics, 27: 2967-2977. https://doi.org/10.1007/s11581-021-04041-w

[6] Shinde, S.S., Kher, J.A. (2014). A review on polyaniline and its noble metal composites. International Journal of Innovative Research in Science, Engineering and Technology, 3(9): 16571-16576. https://doi.org/10.15680/IJIRSET.2014.0310023

[7] Detsri, E., Dubas, S.T. (2013). Interfacial polymerization of polyaniline and its layer-by-layer assembly into polyelectrolytes multilayer thin-films. Journal of Applied Polymer Science, 128(1): 558-565. https://doi.org/10.1002/app.38168

[8] Tan, Y., Liu, Y., Kong, L., Kang, L., Xu, C., Ran, F. (2017). In situ doping of PANI nanocomposites by gold nanoparticles for high-performance electrochemical energy storage. Journal of Applied Polymer Science, 134(38): 45309. https://doi.org/10.1002/app.45309

[9] Vaid, K., Dhiman, J., Kumar, S., Kim, K.H., Kumar, V. (2020). A novel approach for effective alteration of morphological features of polyaniline through interfacial polymerization for versatile applications. Nanomaterials, 10(12): 2404. https://doi.org/10.3390/nano10122404

[10] Zhang, L., Liu, P., Su, Z. (2006). Preparation of PANI-TiO_2 nanocomposites and their solid-phase photocatalytic degradation. Polymer Degradation and Stability, 91(9): 2213-2219. https://doi.org/10.1016/j.polymdegradstab.2006.01.002

[11] Mo, T.C., Wang, H.W., Chen, S.Y., Yeh, Y.C. (2008). Synthesis and dielectric properties of polyaniline/titanium dioxide nanocomposites. Ceramics International, 34(7): 1767-1771. https://doi.org/10.1016/j.ceramint.2007.06.002

[12] Alamgeer, Tahir, M., Sarker, M.R., Ali, S., Ibraheem, Hussian, S., Mohd Said, S. (2023). Polyaniline/ZnO hybrid nanocomposite: Morphology, spectroscopy and optimization of ZnO concentration for photovoltaic applications. Polymers, 15(2): 363. https://doi.org/10.3390/polym15020363

[13] Ahmed, F., Kumar, S., Arshi, N., Anwar, M.S., Koo, B.H., Lee, C.G. (2011). Defect induced room temperature ferromagnetism in well-aligned ZnO nanorods grown on Si (100) substrate. Thin Solid Films, 519(23): 8199-8202. https://doi.org/10.1016/j.tsf.2011.03.062

[14] Noubeil, G., Warda, D., Kamel M. (2020). Extended wide band gap amorphous ZnO thin films deposited by spray pyrolysis. Annales de Chimie Science des Materiaux. 44(5): 347-352. https://doi.org/10.18280/acsm.440507

[15] Poloju, M., Jayababu, N., Reddy, M.R. (2018). Improved gas sensing performance of Al doped ZnO/CuO nanocomposite-based ammonia gas sensor. Materials Science and Engineering: B, 227: 61-67. https://doi.org/10.1016/j.mseb.2017.10.012

[16] Jain, S., Karmakar, N., Shah, A., Shimpi, N.G. (2019). Development of Ni doped ZnO/polyaniline nanocomposites as high response room temperature NO_2 sensor. Materials Science and Engineering: B, 247: 114381. https://doi.org/10.1016/j.mseb.2019.114381

[17] Chen, F., An, W., Li, Y., Liang, Y., Cui, W. (2018). Fabricating 3D porous PANI/TiO_2–graphene hydrogel for the enhanced UV-light photocatalytic degradation of BPA. Applied Surface Science, 427: 123-132. https://doi.org/10.1016/j.apsusc.2017.08.146

[18] Jangid, N.K., Jadoun, S., Yadav, A., Srivastava, M., Kaur, N. (2021). Polyaniline-TiO_2-based photocatalysts for dyes degradation. Polymer Bulletin, 78: 4743-4777. https://doi.org/10.1007/s00289-020-03318-w

[19] Gilja, V., Vrban, I., Mandić, V., Žic, M., Hrnjak-Murgić, Z. (2018). Preparation of a PANI/ZnO composite for efficient photocatalytic degradation of acid blue. Polymers, 10(9): 940. https://doi.org/10.3390/polym10090940

[20] Senapati, A., Chakraborty, A.K. (2021). Flowerlike Fe_2O_3–polyaniline nanocomposite as electrode for supercapacitor. Journal of Materials Science: Materials in Electronics, 32: 27794-27800. https://doi.org/10.1007/s10854-021-07161-1

[21] Yan, J., Wei, T., Fan, Z., Qian, W., Zhang, M., Shen, X., Wei F. (2010). Preparation of graphene nanosheet/carbon nanotube/polyaniline composite as electrode material for supercapacitors. Journal of Power Sources, 195(9): 3041-3045. https://doi.org/10.1016/j.jpowsour.2009.11.028

[22] Shi, L., Wang, X., Lu, L., Yang, X., Wu, X. (2009). Preparation of TiO_2/polyaniline nanocomposite from a lyotropic liquid crystalline solution. Synthetic Metals, 159(23-24): 2525-2529. https://doi.org/10.1016/j.synthmet.2009.08.056

[23] Mostafaei, A., Zolriasatein, A. (2012). Synthesis and characterization of conducting polyaniline nanocomposites containing ZnO nanorods. Progress in Natural Science: Materials International, 22(4): 273-280. https://doi.org/10.1016/j.pnsc.2012.07.002

[24] Jing, Y., Lai, Y., Zhang, S., Wang, R., Xu, Z., Pei, Y. (2021). The adsorption performance of polyaniline/ZnO synthesized through a two-step method. Crystals, 12(1): 34. https://doi.org/10.3390/cryst12010034

[25] Mutlaq, S., Albiss, B., Al-Nabulsi, A.A., Jaradat, Z.W., Olaimat, A.N., Khalifeh, M.S., Holley, R.A. (2021). Conductometric immunosensor for Escherichia coli O157: H7 detection based on polyaniline/zinc oxide

(PANI/ZnO) nanocomposite. Polymers, 13(19): 3288. https://doi.org/10.3390/polym13193288
[26] Andreas, R., Lesbani, A., Yusuf, F.A. (2019). The character istics (compositions, morphological, and structure) of nanocomposites polyaniline (PANI)/ZnO. In IOP Conference Series: Materials Science and Engineering, 509(1): 012126. https://doi.org/10.1088/1757-899X/509/1/012126
[27] Turkten, N., Karatas, Y., Bekbolet, M. (2021). Preparation of PANI modified ZnO composites via different methods: Structural, morphological and photocatalytic properties. Water, 13(8): 1025. https://doi.org/10.3390/w13081025
[28] Eskizeybek, V., Sarı, F., Gülce, H., Gülce, A., Avcı, A. (2012). Preparation of the new polyaniline/ZnO nanocomposite and its photocatalytic activity for degradation of methylene blue and malachite green dyes under UV and natural sun lights irradiations. Applied Catalysis B: Environmental, 119: 197-206. https://doi.org/10.1016/j.apcatb.2012.02.034
[29] Somani, P.R., Marimuthu, R., Mulik, U.P., Sainkar, S.R., Amalnerkar, D.P. (1999). High piezoresistivity and its origin in conducting polyaniline/TiO_2 composites. Synthetic Metals, 106(1): 45-52. https://doi.org/10.1016/S0379-6779(99)00081-8
[30] Niu, Z., Yang, Z., Hu, Z., Lu, Y., Han, C.C. (2003). Polyaniline–silica composite conductive capsules and hollow spheres. Advanced Functional Materials, 13(12): 949-954. https://doi.org/10.1002/adfm.200304460
[31] Chufamo, S., Kelita, B., Lelago, A., Kemal, A. (2022). Multilayered electroactive polyaniline-ZnO composite films fabricated electrode for voltammetric determination of paracetamol. Systematic Reviews in Pharmacy, 13(8): 791-797. https://doi.org/10.31858/0975-8453.13.8.791-797
[32] He, Y. (2005). A novel emulsion route to sub-micrometer polyaniline/nano-ZnO composite fibers. Applied Surface Science, 249(1-4): 1-6. https://doi.org/10.1016/j.apsusc.2004.11.061.
[33] Paul, G.K., Bhaumik, A., Patra, A.S., Bera, S.K. (2007). Enhanced photo-electric response of ZnO/polyaniline layer-by-layer self-assembled films. Materials Chemistry and Physics, 106(2-3): 360-363. https://doi.org/10.1016/j.matchemphys.2007.06.013
[34] Patil, S.L., Pawar, S.G., Chougule, M.A., Raut, B.T., Godse, P.R., Sen, S., Patil, V.B. (2012). Structural, morphological, optical, and electrical properties of PANi-ZnO nanocomposites. International Journal of Polymeric Materials, 61(11): 809-820. https://doi.org/10.1080/00914037.2011.610051
[35] Li, J., Qiu, S., Liu, B., Chen, H., Xiao, D., Li, H. (2021). Strong interaction between polyaniline and carbon fibers for flexible supercapacitor electrode materials. Journal of Power Sources, 483: 229219. https://doi.org/10.1016/j.jpowsour.2020.229219